www.elsevier.nl/locate/carres

Carbohydrate Research 328 (2000) 103–113

CARBOHYDRATE
RESEARCH

Interaction of saccharides with rare earth metal ions: synthesis and characterisation of Pr(III)– and Nd(III)–saccharide complexes

Anindita Mukhopadhyay [a], Erkki Kolehmainen [b], Chebrolu P. Rao [a,*]

[a] *Department of Chemistry, Bioinorganic Laboratory, Indian Institute of Technology, Powai, Mumbai, Bombay 400 076, India*

[b] *Department of Chemistry, Jyvaskyla University, Jyvaskyla Fin-40351, Finland*

Received 17 December 1999; accepted 13 March 2000

Abstract

A number of complexes are synthesised with Pr(III) and Nd(III) employing the mono- and disaccharides, D-glucose, D-galactose, D-mannose, D-arabinose, D-ribose, D-xylose, maltose and lactose. The complexes are characterised by various spectral and analytical techniques, and based on these data, appropriate structures were assigned for all complexes. © 2000 Elsevier Science Ltd. All rights reserved.

Keywords: Rare earth metal ions; Saccharides; ^{13}C NMR; Pr(III)–saccharide complexes, Nd(III)–saccharide complexes; Chelation by saccharides; Metal-ion induced ^{13}C NMR shifts ($\Delta\delta$)

---

1. Introduction

Saccharides and their derivatives, are important molecular components present in chemical, biological and industrial processes. Studies concerned with the synthesis, isolation and characterisation of transition metal–saccharide complexes have been addressed extensively in the literature in recent years [1]. However, knowledge regarding the interactions of saccharides with rare earth elements is rather limited in the literature, in spite of the fact that such studies would have a great influence on the growth of metal–saccharide chemistry [2,3]. In continuation with our ongoing efforts in developing metal–saccharide chemistry in general, and rare-earth metal ion–saccharide chemistry in particular [4], this paper deals with the study of the synthesis and characterisation of isolated products of Pr(III) and Nd(III) with different mono- and disaccharides.

2. Experimental

Methods and materials.—MeOH and acetone were purified, dried and distilled prior to use by the usual methods. All the saccharides and sodium metal were purchased from Aldrich (USA) or Lancaster Synthesis (UK) and used without further purification. Hydrated Pr(III) and Nd(III) chlorides were prepared from the respective oxides by adapting a literature procedure [5].

Absorption spectra were recorded using a Shimadzu UV-2101 spectrophotometer. FTIR

---

* Corresponding author. Tel.: +91-22-5767162/5722545; fax: +91-22-5723480/5767152.

E-mail address: cprao@ether.chem.iitb.ernet.in (C.P. Rao).

PII: S0008-6215(00)00084-7

spectra were recorded in KBr matrix on an Impact 400 Nicolet FTIR spectrometer. Elemental analyses were performed on a Carlo–Erba elemental analyser. Praseodymium, neodymium and sodium contents were determined using inductively coupled plasma–atomic emission spectroscopy (ICP–AES) Labtam Plasmalab 8440 analyser. CD experiments were performed on a JASCO J-600 spectropolarimeter. Thermal analysis was performed on a Shimadzu DT-30 thermal analyser. Cyclic voltammetry was carried out on a BAS-100 electrochemical analyser. NMR studies were performed on a Bruker Advance DRX500 spectrometer. All the solution characterisations were performed with freshly prepared aqueous solutions of the complexes

Synthesis.—All the complexes were synthesised using a similar procedure. One typical procedure is given below for the synthesis of the D-glucose complex of Pr(III).

Pr(III)–D-Glc (1). D-glucose (0.720 g, 4 mmol) was suspended in 60 mL of MeOH and stirred for 30 min. Freshly cut sodium metal (0.184 g, 8 mmol) was added to it with stirring, while keeping the reaction mixture in an ice–salt bath. Stirring was continued for a further 3–4 h until it formed a white suspension in MeOH. The sodium salt suspension was brought to room temperature, and $PrCl_3 \cdot 6\ H_2O$ (0.355 g, 1 mmol) dissolved in 5 mL of MeOH was added dropwise to it. The resulting suspension was allowed to stir for a further 4 h to give a light-yellow coloured solid. The solid was then filtered, washed twice with a 1:10 water–MeOH mixture, followed by thrice with acetone. The product was finally dried under vacuum for several hours to obtain an off-white solid in 45% yield.

All the other monosaccharide complexes, Pr–D-galactose (**2**); Pr–D-mannose (**3**); Pr–D-arabinose (**4**); Pr–D-ribose (**5**) and Pr–D-xylose (**6**) were prepared and isolated using the same procedure. The disaccharide compounds Pr–D-maltose (**7**) and Pr–D-lactose (**8**) were also prepared by adapting the same procedure, but using 0.720 g (2 mmol) of disaccharide, 0.184 g (8 mmol) of sodium metal and 0.355 g (1 mmol) of $PrCl_3 \cdot 6\ H_2O$ in 50 mL of MeOH. Nd(III) complexes, Nd–D-glucose (**9**); Nd–D-galactose (**10**); Nd–D-mannose (**11**); Nd–D-arabinose (**12**); Nd–D-ribose (**13**); Nd–D-xylose (**14**); Nd–D-maltose (**15**) and Nd–D-lactose (**16**) were prepared adapting the same procedure, but using $NdCl_3 \cdot 6H_2O$. These complexes were isolated and purified in a similar manner to obtain off-white solids. The yields obtained for all the complexes were in the range 45–75%.

3. Results and discussion

There observed similarities in the physical and chemical properties of Pr(III)–saccharide complexes (**1**–**8**) and Nd(III)–saccharide complexes (**9**–**16**). All the complexes were found to be soluble in warm water, but not in any common organic solvents. The compounds were stable in the solid state for several weeks if kept protected from moisture. However in moist conditions, the compounds form a dark-coloured pasty mass in about 5–6 days. The aqueous solutions of the complexes were found to be stable for 4–5 days, after which a gradual decrease was observed in the intensities of the charge-transfer bands over the next 4–5 days, indicating their slow hydrolysis. Therefore, all the aqueous solution characterisations were performed using freshly prepared solutions. Aqueous solutions of all the complexes have exhibited good ionic conductivity. Also compounds **1**–**16** were analysed for elemental compositions. Both elemental analysis data and molar conductance data are listed in Table 1 for all the complexes.

Thermal analysis.—Thermal degradation of Pr(III)– and Nd(III)–saccharide complexes showed three main steps. The thermal analysis data with appropriate assignments of the fragments is listed in Table 2 for all the complexes **1**–**16**. In the temperature range 50–150 °C, the solvent molecules were lost and in the range 150–220 °C. Mainly CO_2 and some amount of H_2O molecules were found to be lost. The pyrolysis of the main saccharide framework starts in this temperature range and continues up to about 450 °C. Evolution of CO and H_2O were the main features observed in the higher temperature range ($>$ 220 °C) in a number of steps. The degradation patterns were found to be similar, even with several other metal-bound saccharide complexes [6,7].

FTIR studies.—FTIR spectra of all the complexes (**1**–**16**) were measured in KBr matrix in the range 400–4000 cm^{-1}. The spectra have shown usual line broadening as expected in cases of metal-bound saccharide moieties. In Fig. 1, selected spectra of the ligands and the corresponding complexes of both Pr(III) and Nd(III) were shown for effective comparison. Spectral features of these complexes closely resemble those observed earlier in the case of Ce(III)–saccharide complexes [4]. A broad, intense band observed around 3400 cm^{-1} is assignable to an O–H stretching vibration. Peaks observed around 2850 cm^{-1} are assignable to the asymmetric C–H stretching vibrations. The C–C and C–O stretching vibrations appeared at ~1600 and ~1400 cm^{-1}, respectively. The –OCH and –CCH bending vibrations are observed at ~1050 cm^{-1}. Thus the FTIR spectra have clearly indicated the binding of saccharide moieties to Pr(III) or Nd(III) centres in products **1**–**16**, suggesting that the products are metal-ion bound complexes.

Table 1
Composition, formula, analyses and conductance data of complexes **1**–**16**

Compound no. and title	Composition and formula	Analysis [a]				Molar conductance (ohm^{-1} M^{-1} cm^2)
		%C	%H	%Na	%M	
1	$C_{13}H_{36}Na_3O_{20}Pr$	*C* 28.73	4.57	8.68	17.74	167
(Pr–D-Glu)	$Na_3[Pr(D\text{-}Glc)_3]\cdot CH_3OH\cdot H_2O$	*O* 28.94	3.52	8.59	17.05	
2	$C_{18}H_{34}Na_3O_{20}Pr$	*C* 27.71	4.39	8.84	18.06	169
(Pr–D-Gal)	$Na_3[Pr(D\text{-}Gal)_3]\cdot 2\ H_2O$	*O* 27.05	3.70	8.44	17.56	
3	$C_{21}H_{38}Na_3O_{20}Pr$	*C* 30.75	4.67	8.41	17.18	175
(Pr–D-Man)	$Na_3[Pr(D\text{-}Man)_3]\cdot CH_3COCH_3\cdot H_2O$	*O* 29.76	4.09	7.98	16.56	
4	$C_{16}H_{30}Na_3O_{17}Pr$	*C* 27.29	4.29	9.79	20.00	149
(Pr–D-Ara)	$Na_3[Pr(D\text{-}Ara)_3]\cdot CH_3OH\cdot H_2O$	*O* 27.62	3.72	9.36	18.99	
5	$C_{15}H_{28}Na_3O_{17}Pr$	*C* 26.10	4.09	9.99	20.41	187
(Pr–D-Rib)	$Na_3[Pr(D\text{-}Rib)_3]\cdot 2\ H_2O$	*O* 26.77	3.99	9.58	19.58	
6	$C_{18}H_{32}Na_3O_{17}Pr$	*C* 29.60	4.42	9.44	19.29	182
(Pr–D-Xyl)	$Na_3[Pr(D\text{-}Xyl)_3]\cdot CH_3COCH_3\cdot H_2O$	*O* 30.02	3.65	8.87	18.80	
7	$C_{25}H_{46}Na_3O_{24}Pr$	*C* 33.62	4.81	7.15	14.61	205
(Pr–D-Mal)	$Na_3[Pr(D\text{-}Mal)_2]\cdot CH_3OH\cdot 2\ H_2O$	*O* 32.98	4.44	6.84	14.40	
8	$C_{25}H_{46}Na_3O_{24}Pr$	*C* 33.62	4.81	7.15	14.61	195
(Pr–D-Lac)	$Na_3[Pr(D\text{-}Lac)_2]\cdot CH_3OH\cdot 2\ H_2O$	*O* 33.17	4.62	6.92	14.05	
9	$C_{19}H_{38}Na_3NdO_{21}$	*C* 27.98	4.70	8.46	17.68	179
(Nd–D-Glu)	$Na_3[Nd(D\text{-}Glc)_3]\cdot CH_3OH\cdot 2\ H_2O$	*O* 28.24	5.35	8.32	16.91	
10	$C_{21}H_{38}Na_3NdO_{20}$	*C* 30.63	4.65	8.37	17.51	201
(Nd–D-Gal)	$Na_3[Nd(D\text{-}Gal)_3]\cdot CH_3COCH_3\cdot H_2O$	*O* 29.96	3.65	7.98	16.61	
11	$C_{18}H_{34}Na_3NdO_{20}$	*C* 27.59	4.37	8.80	18.41	158
(Nd–D-Man)	$Na_3[Nd(D\text{-}Man)_3]\cdot 2\ H_2O$	*O* 28.23	4.05	8.22	17.68	
12	$C_{16}H_{34}Na_3NdO_{19}$	*C* 25.84	4.61	9.27	19.40	169
(Nd–D-Ara)	$Na_3[Nd(D\text{-}Ara)_3]\cdot CH_3OH\cdot 3\ H_2O$	*O* 26.17	3.93	8.98	18.87	
13	$C_{18}H_{32}Na_3NdO_{17}$	*C* 29.47	4.40	9.40	19.66	172
(Nd–D-Rib)	$Na_3[Nd(D\text{-}Rib)_3]\cdot CH_3COCH_3\cdot H_2O$	*O* 30.03	3.97	9.15	18.78	
14	$C_{19}H_{36}Na_3NdO_{18}$	*C* 29.80	4.75	9.01	18.84	162
(Nd–D-Xyl)	$Na_3[Nd(D\text{-}Xyl)_3]\cdot CH_3COCH_3\cdot CH_3OH\cdot H_2O$	*O* 29.77	4.60	8.79	18.00	
15	$C_{24}H_{42}Na_3NdO_{24}$	*C* 31.07	4.56	7.43	15.55	197
(Nd–D-Mal)	$Na_3[Nd(D\text{-}Mal)_2]\cdot 2\ H_2O$	*O* 30.93	4.61	7.15	14.92	
16	$C_{24}H_{42}Na_3NdO_{24}$	*C* 31.07	4.56	7.43	15.55	201
(Nd–D-Lac)	$Na_3[Nd(D\text{-}Lac)_2]\cdot 2\ H_2O$	*O* 30.86	4.76	7.22	14.78	

[a] *C* represents calculated and *O* represents the observed values.

Table 2
Thermal analysis data of complexes **1**–**16**

Compound	*T* (°C)	% Weight loss	Possible fragments
1	75; 160; 285; 390; 440	4; 9; 23; 18; 12	CH_3OH; CO_2+H_2O; 4 CO+2.5 H_2O; 2(CO+H_2O); 2 CO
2	105; 220; 295; 360; 455	5; 17; 22; 19; 13	2 H_2O; 3 CO_2; 4 CO+1.5 H_2O; 3 CO; 2 CO
3	60; 102; 240; 285; 370; 410	7; 8; 12; 24; 25; 7	CH_3COCH_3; CO_2+H_2O; 2 CO_2; 4 CO+2 H_2O; 4 CO; CO
4	70; 190; 230; 385; 450	5; 9; 18; 23; 17	CH_3OH; CO_2+H_2O; 3 CO+1.5 H_2O; 4 CO; 2 CO+0.5 H_2O
5	95; 185; 255; 290; 400	4.5; 9; 18; 23; 15	1.5 H_2O; CO_2+H_2O; 2 CO+3 H_2O; 3 CO+2 H_2O; 2 CO
6	70; 165; 265; 380; 410	8; 10; 15; 21; 18	CH_3COCH_3; CO_2+H_2O; 3 CO+0.5 H_2O; 3.5 CO+0.5 H_2O; 2.5 CO
7	75; 156; 260; 390; 410	3.5; 18; 24; 21; 15	CH_3OH; 3 CO_2+2 H_2O; 5 CO+2 H_2O; 4.5 CO; 2.5 CO
8	55; 125; 190; 265; 370; 435	3.5; 9; 18; 25; 21; 5	CH_3OH; CO_2+2 H_2O; 5 CO+0.5 H_2O; 6 CO; 4 CO; CO
9	70; 160; 190; 260; 380; 400	4; 10; 18; 20.5; 18.5; 9	CH_3OH; CO_2+2 H_2O; 4 CO_2+H_2O; 4.5 CO; 3 CO; 1.5 CO
10	90; 190; 255; 350; 365; 460	10; 12; 21; 18.5; 12; 8	$CH_3COCH_3+H_2O$; 2 CO_2; 4 CO+1.5 H_2O; 3 CO+0.5 H_2O; 2 CO, CO
11	100; 210; 250; 350; 420	5; 13; 22; 18; 12	2 H_2O; 2 CO_2+0.5 H_2O; 5 CO; 3 CO; 2 CO
12	70; 200; 280; 350; 460	7; 18.5; 21; 11; 7	CH_3OH; 3(H_2O+CO_2); 4 CO+H_2O; 2 CO; CO
13	50; 105; 295; 270; 385; 410	8; 3.5; 11; 18.5; 12; 9	CH_3COCH_3; 2 H_2O; 2 CO_2; 4 CO+H_2O; 2 CO; 2 CO
14	90; 105; 200; 280; 360; 420	12; 3.5; 11; 22; 18; 8	$CHCOCH_3+CH_3OH$; H_2O; 2 CO_2; 4 CO+H_2O; 3 CO; CO
15	105; 190; 220; 350; 430	4; 13; 25; 22; 13	2 H_2O; 2 CO_2+1.5 H_2O; 7 CO; 4.5 CO; 2 CO
16	110; 200; 280; 365; 425	3.5; 15; 20; 25; 12	2 H_2O; 3 CO_2; 5 CO+H_2O; 5.5 CO; 2 CO

Solution absorption and solid-state diffused reflectance spectra.—The aqueous solution absorption spectra were measured in the range 190–900 nm. The electronic transitions in lanthanides are expected to show sharp signals, as the perturbation caused due to external fields is minimum in the case of the deep-seated f-orbital. However, a broad spectral pattern can be observed in the case of the ligand-to-metal charge-transfer transitions in rare earth metal ions. The absorption spectral behaviour observed with our complexes is comparable with that reported in the literature, in the case of lanthanide complexes [8].

In the case of Pr(III) complexes **1**–**8**, somewhat sharper signals were observed in the visible region [400–900 nm, Fig. 2(b)] at around, 585, 480, 465 and 445 nm, assignable to the possible f → f transitions in the complexes (Table 3). When a lanthanide ion is doped in some host lattice, a large number of very sharp f → f transitions ($\Delta\lambda_{1/2} = 0.05$–0.2 nm) occur due to the existence of a number of microstates arising from a given f^n configuration [9]. But when the ion is in solution in the presence of some ligand, the number of transitions will be less because of the merging of some of the sharper signals, which results in a broad band with a larger bandwidth. In the case of the aqueous solution of Pr(III)– and Nd(III)–saccharide complexes the f → f transitions were found to be broad by about 100-fold (5–20 nm), when compared to the sharp spectra of doped ions. However the f → f transition bands are much sharper than the d → d transitions found in the corresponding transition metal–saccharide complexes. The d→d electronic transitions were found to be at least ten times broader ($\Delta\lambda_{1/2} = \sim 150$ nm for Cr^{3+}, ~100 nm for VO^{2+}, ~80 nm for Co^{2+} and ~120 nm for Ni^{2+}) than those of the f→f ones observed in the present case [10]. Even the aqueous solution spectrum of the corresponding $LnCl_3$ was found to be similar but only with a marginal lowering of the bandwidths. Comparison of the f→f electronic transition spectra of doped Pr(III) with those of the Pr(III)–saccharide complexes in aqueous solution indicated that the observed transitions in case of **1**–**8** can be assigned to $^3H_4 \rightarrow {}^1D_2$, $^3H_4 \rightarrow {}^1I_1$, $^3H_4 \rightarrow {}^3P_1$ and $^3H_4 \rightarrow {}^3P_2$, respectively, where the ground state for the f^2 ion is $^3H_4$. At least two to three very broad charge-transfer bands (saccharide–O^- to Pr^{3+}) were observed in the case of complexes **1**–**8** in the range 250–350 nm, as shown in Fig. 2(a).

In the case of Nd(III) complexes, sharp bands were observed at around 860, 800, 740, 670, 570, 515 and 460 nm, as shown in Fig. 2(d). In the case of Nd(III) (f^3 system), the number of microlevels as well as the allowed transitions are much higher than those in the case of Pr(III), (f^2 system) among which some of the strongest ones are observable. In the case of Nd(III) complexes **9**–**16**, in aqueous solutions the f→f transition were assignable to $^4I_{9/2} \rightarrow {}^2H_{3/2}$, $^4I_{9/2} \rightarrow {}^2H_{9/2}$, $^4I_{9/2} \rightarrow {}^4S_{3/2}$, $^4I_{9/2} \rightarrow {}^4F_{9/2}$, $^4I_{9/2} \rightarrow {}^2G_{5/2}$, $^4I_{9/2} \rightarrow {}^2G_{9/2}$ and $^4I_{9/2} \rightarrow {}^4G_{11/2}$, when compared to the spectra of the doped ion, where the ground state of the ion is $^4I_{9/2}$. However, the f→f transitions observed in **9**–**16** were found to be broader by a factor of two (Fig. 2(b) and (d)) when compared to those of **1**–**8**. Absorption band positions obtained in the range 450–700 nm in the present case, have close relevance with the features obtained for Nd(III)–porphyrinato double-decker complexes reported in the literature [11]. At least three to four very broad charge-transfer bands (saccharide–O^- to Nd^{3+}) were observed in the case of **9**–**16** in the range 250–400 nm as shown in Fig. 2(c).

The diffused reflectance spectra of all the complexes were found to be essentially similar to those observed in fresh solution, thereby

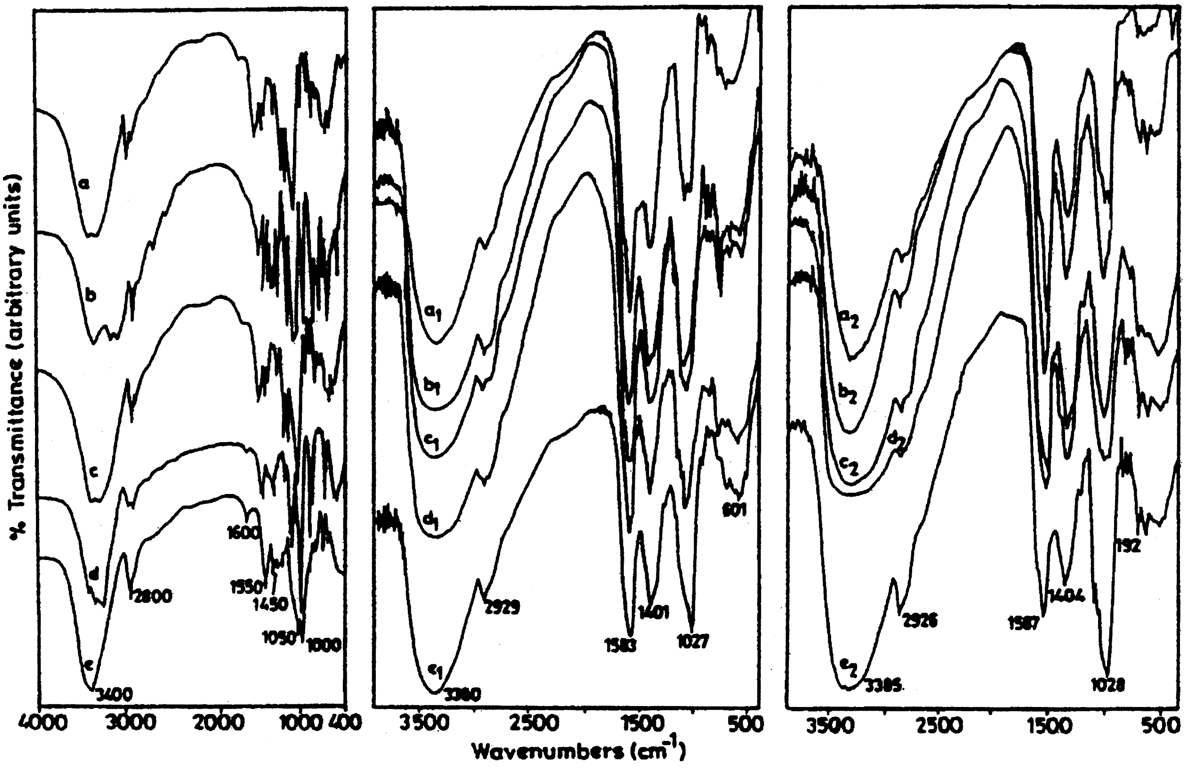

Fig. 1. FTIR spectra of (a) D-glucose; (b) D-mannose; (c) D-arabinose; (d) D-xylose; (e) D-maltose; (a_1) **1**, Pr–D-glucose; (b_1) **3**, Pr–D-mannose; (c_1) **4**, Pr–D-arabinose; (d_1) **6**, Pr–D-xylose; (e_1) **7**, Pr–D-maltose; (a_2) **9**, Nd–D-glucose; (b_2) **11**, Nd–D-mannose; (c_2) **12**, Nd–D-arabinose (d_2) **14**, Nd–D-xylose and (e_2) **15**, Nd–D-maltose.

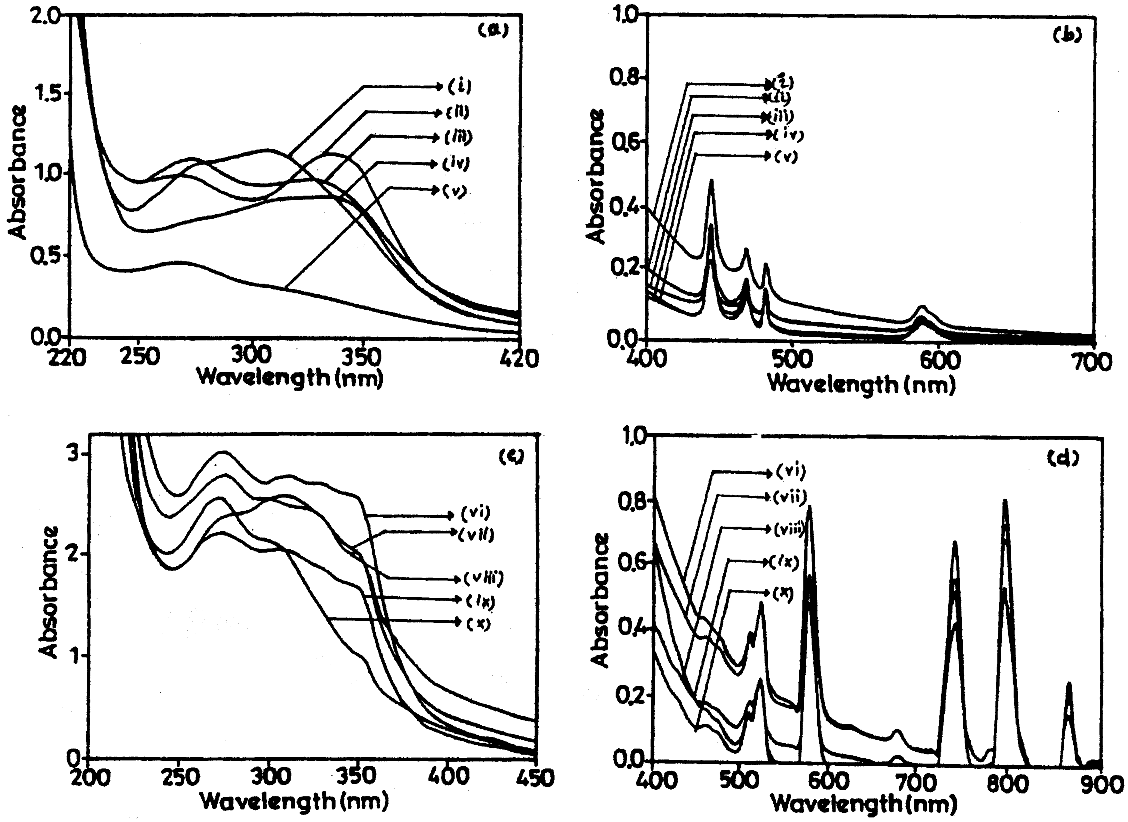

Fig. 2. Aqueous solution absorption spectra of some of the complexes in the UV and visible regions: (a) and (b) represent Pr(III) complexes, and (c) and (d) represent Nd(III) complexes. (i) **1**; (ii) **3**; (iii) **4**; (iv) **6**; (v) **7**; (vi) **9**; (vii) **11**; (viii) **12**; (ix) **14** and (x) **15**.

indicating the retainment of the solid-state structure upon dissolution.

Magnetic susceptibility measurements.— Room temperature magnetic susceptibility measurements of the powdered samples showed magnetic moment (μ_{eff}) values in the range 3.30–3.95 μ_B for all complexes **1**–**16**. These are found to be higher than their spin only values (2.83 and 3.87 μ_B, respectively, for f^2 and f^3 systems). In the case of lanthanide ions it is generally expected that the value of the magnetic moment is higher than the spin-only value due to the orbital contribution [12], and the magnitude of the orbital contribution is found to be decreased as the number of f-electrons increases in the series. Thus the magnetic susceptibility studies have strongly suggested the presence of praseodymium and neodymium ions in their + 3 oxidation states in all these complexes.

Circular dichroism.—CD spectra of aqueous solutions of the complexes were measured in the UV region. Though the Cotton effect is not prominent here, as was observed in the case of the Ce(III)–saccharide complexes, the trends among different complexes are appreciable. The glucose complexes exhibit a CD sign which is opposite to the other hexose complexes of the corresponding metal ion. For example, the Nd–glucose complex **9**, exhibited a CD sign that is opposite to that of Nd–galactose complex **10** as shown in Fig. 3(a). Similarly the xylose complex exhibits a CD sign which is opposite to the other pentose complexes of the same metal ion. For example, Nd–xylose complex **14**, exhibited a CD sign which is opposite to that of Nd–arabinose complex **12**, as shown in Fig. 3(b). Among the disaccharide complexes, maltose complexes **7** and **15** have shown the same CD sign as that of glucose complexes **1** and **9**, whereas lactose complexes **8** and **16** have shown the same CD sign as that of the galactose complexes **2** and **10**. The CD spectra of Nd(III) complexes **9**, **10**, **15** and **16** are shown in Fig. 3(a). This in turn indicates that the disaccharides interact with the metal ions predominantly through the non-reducing part and further retains the configuration of their non-reducing fragment in the complexes. Similar trends were observed in the sign of the CD spectra of the Mo(VI)– and Ce(III)–saccharide complexes [4,7]. The studies indicated that there seems to exist certain preferential orientations for different saccharides in their binding to metal ions.

Cyclic voltammetry.—Cyclic voltammograms of all the complexes were measured in 0.1 M aqueous KCl, using Pt as the working electrode and Ag/AgCl as the reference electrode, in an atmosphere of argon, with a scan speed range of 60–100 mV s^{-1}. Voltammetric responses corresponding to Ln(III) → Ln(II) were irreversible and were found in the positive potential range in all cases. Voltammograms of **1**, **7**, and **10** are shown in Fig. 4. Individual responses were observed at, + 350, + 505, + 450, + 480, + 390, + 520, + 550, + 495, + 560, + 400, + 395, + 415, + 360, + 350, + 520 and + 460, respectively, for complexes **1**–**16**. The study indicated the instability of the corresponding reduced species, Pr(II) or Nd(II) in solution. A close comparison of these potentials could not be made due to paucity of the literature dealing with the CV studies of somewhat similar systems. However, recently studied lanthanide–porphyrinato double-decker complexes have all exhibited only ligand-based, reversible redox couples [11]. Although, in the case of monophthalocyanine complexes of rare earth ions, an oxidation couple was observed at + 0.6 V (vs. SCE) and a reduction couple was observed at around − 1.0 V (vs. SCE); the origin of these were unassigned [13].

Nuclear magnetic resonance studies.—^{13}C NMR spectra of the complexes and those of the free saccharides were measured in aqueous

Table 3
UV–Vis spectral data of complexes **1**–**16**

Compound	$\lambda(\varepsilon)$, nm (L M^{-1} cm^{-1})
1	590(5), 478(10), 465(12), 446(25), 340(6350), 306(6432), 272(5454)
2	587(5), 480(12), 467(14), 445(24), 332(1610), 273(1885)
3	590(4), 482(8), 469(10), 443(19), 337(6630), 270(3800)
4	589(4), 482(7), 469(9), 444(19), 344(3850), 306(6270), 273(5620)
5	588(5), 481(8), 468(9), 444(18), 332(3760), 273(4400)
6	590(3), 483(6), 465(7), 442(15), 3298(1570), 269(3000)
7	588(6), 481(12), 468(14), 444(26), 339(4660), 269(5340)
8	585(5), 480(11), 468(13), 446(25), 338(5986), 271(6470)
9	864(12), 795(44), 735(29), 570(32), 520(22), 512(12), 348(1300), 308(1640), 271(1500)
10	864(28), 794(14), 740(54), 575(53), 521(53), 511(34), 322(3000), 272(3525)
11	865(34), 794(43), 740(71), 575(73), 521(46), 511(22), 327(2693), 268(3414)
12	865(17), 794(60), 740(50), 575(41), 522(25), 512(12), 306(5000), 276(2890)
13	861(22), 789(64), 736(52), 572(61), 518(45), 508(30), 309(4000), 275(3683)
14	863(30), 790(80), 745(64), 519(38), 510(18), 323(2580), 270(2940)
15	860(27), 789(90), 742(56), 576(56), 521(32), 511(14), 306(3200), 271(3650)
16	861(32), 790(22), 739(65), 573(52), 519(45), 505(24), 305(3960), 274(3754)

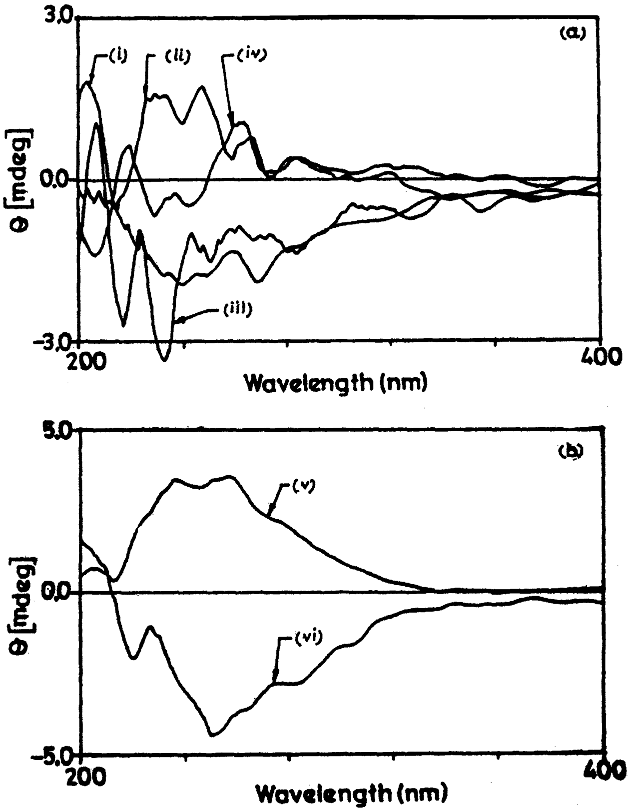

Fig. 3. Aqueous solution CD spectra of some of the Nd(III) complexes: (a): (i) **9**; (ii); **10** (iii) **15**; (iv) **16**; and (b): (v) **12** and (vi) **14**.

solution. Complexation shifts ($\Delta\delta = \delta_{\text{complex}} - \delta_{\text{ligand}}$, metal induced shifts) were observed in each of the carbon atoms and are listed in Table 4. It has been found that pyranose conformation was predominant in the spectra of all the free saccharides. However, in the metal–saccharide complexes, it is the furanose form that was found to be the major one, at least in some cases.

Pr(III) complexes.—Among the monosaccharide complexes, **1**, **2**, **3** and **4** have shown significantly high complexation shifts (metal-induced shifts) at C-3 and C-4, whereas **5** and **6** have shown such shifts at C-2 and C-3. Also it has been found that the saccharides in **5** and **6** are in interaction with the metal ion predominantly through furanose form ($\Delta\delta$, Table 4). Based on the magnitude of the $\Delta\delta$ values, additional interactions were predicted for complexes **1**, **2** and **4** through OH-2; complex **3**, through OH-1 and complexes **5** and **6** through OH-4. In the case of disaccharide complexes **7** and **8**, significantly high complexation shifts ($\Delta\delta$ values) were observed with C-3′, C-4′ and C-2′ for maltose, and C-3′, C-4′ and C-3 for the lactose complexes. Weak in-

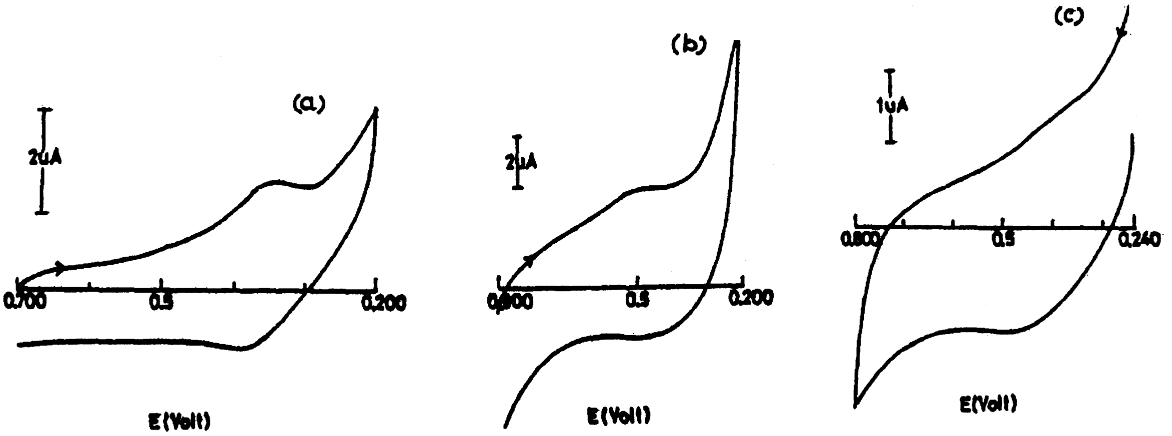

Fig. 4. Cyclic voltammograms of some of the complexes, (a) **1**; (b) **7**, and (c) **10** in 0.1 M aqueous KCl, using Ag/AgCl as the reference electrode and Pt as the working electrode.

Table 4
Complexation shift ($\Delta\delta$) values for complexes **1**–**16**

Compound	C-1		C-2		C-3		C-4		C-5		C-6	
1	4.69		7.59		6.46		8.25		3.71		2.21	
2	4.19		5.54		9.57		5.18		7.00		1.18	
3	6.47		4.21		7.01		6.77		3.72		0.89	
4	3.74		4.19		3.67		6.11		1.18		–	
5	3.66		7.59		6.32		5.22		0.11		–	
6	4.37		8.66		6.15		8.21		1.64		–	
9	3.82		3.58		6.15		4.45		4.47		0.15	
10	3.85		1.32		6.10		6.75		4.53		0.15	
11	4.4		3.59		8.87		10.03		1.80		4.09	
12	0.40		1.69		3.10		9.25		1.65		–	
13	0.29		1.65		5.88		6.17		2.57		–	
14	4.40		0.78		10.02		8.87		1.68		–	
	C-1′ [a]	C-1	C-2′	C-2	C-3′	C-3	C-4′	C-4	C-5′	C-5	C-6′	C-6
7	4.63	1.47	6.64	1.36	8.75	3.40	9.61	0.24	2.83	2.87	1.11	1.11
8	X [b]	X	5.49	4.67	8.75	6.47	10.17	0.49	3.36	1.73	1.12	1.00
15	1.59	1.25	4.32	2.84	7.26	7.00	10.50		4.70	3.33	1.18	0.65
16	4.00	7.68	3.23	4.90	5.14	3.18	10.58		3.09	3.07	0.64	0.26

[a] C′ indicates the carbon atoms from the non-reducing part of the disaccharides.

[b] X means the value could not be obtained.

teractions extended by the –OH groups were predicted to be through OH-2 and OH-3 for maltose, and OH-6′ and OH-1 for lactose complexes.

Nd(III) complexes.—All the monosaccharide complexes among **9**–**14** have exhibited significantly high complexation shifts ($\Delta\delta$, Table 4) with C-3 and C-4 centres. Both ribose and xylose have been shown to interact with the Nd(III) centre through the pyranose form. Apart from that, a considerable $\Delta\delta$ value was observed with C-1 in the case of **9**, **10**, **11** and **14**, and with C-2 in the case of **12** and **13**. The disaccharide complex **15** has exhibited fairly major shifts in C-3′, C-4′ and C-3, followed by C-2′ and C-2. Similarly, **16** has exhibited considerably major shifts with the C-3′, C-4′ and C-1 centres, followed by C-2′ and C-3. Based on the $\Delta\delta$ values given in Table 4, it has been possible to identify the –O$^-$ and –OH moieties involved in binding. While generally larger $\Delta\delta$ values are attributed to arise from –O$^-$ binding, importance was also given to identify those adjacent –OH groups capable of showing bidentate chelation. However, generally smaller $\Delta\delta$ values are assigned to those –OH groups weakly interacting with the metal-ion centres, without deprotonation. In the case of a pyranose structure, the shift obtained for C-5 is attributable to the electric and magnetic through-space effect of the metal ion, as proposed in the literature [14].

4. Conclusions and correlations

The molar conductance data (Table 1) is clearly indicative of a 3:1 electrolyte in all complexes **1**–**16**. The elemental analysis data (Table 1) revealed that in all the complexes, metal ions are associated with either three monosaccharides or two disaccharides. In the binding of two disaccharide molecules per metal ion, a new observation has been found, only in the case of Pr(III) and Nd(III) complexes, and has not been found with any saccharide complexes reported earlier [1,4,7]. Thermal degradation studies have helped to determine the presence of solvent molecules. These studies have also elicited the pyrolysis process of saccharide moieties present in the complexes. It has been noted in recent literature that Eu(III) binds with two molecules of cyclohexanetriol (as tridentate) along with one or two chelating nitrates and water molecules to crystallise predominantly to give a nine-coordinated, tricapped trigonal prismatic complex [15]. Also it has been found in the literature, that saccharides can bind to metal ions as tridentate chelate as well as in a tri- or tetradentate bridging manner [16]. All the data collected and analysed in the present case are characteristic of the presence of Pr and Nd ions in their +3 oxidation state, and similarities have been noted between the data for the complexes of Pr(III) and Nd(III). Subtle differences existing in the conformation as well as the binding mode of saccharide molecules, have been elucidated based on ^{13}C NMR studies. Ribose and xylose complexes of Pr(III) have adopted a furanose conformation, while those of Nd(III) have adopted a pyranose one as shown in Fig. 5(b) and (c). In the case of Mo(VI)– and Ce(III)–ribose and –xylose complexes, the pyranose form was found to interact with the metal ions [4,7]. But in the case of the complexes of the first-row transition-metal ions, the predominant conformation was furanose for ribose and xylose [17]. Based on analytical and spectral data of these complexes, all these complexes have been found to have a complex anion of the type, $[M(sacc)_3]^{3-}$ for monosaccharides (**1**–**6** and **9**–**14**), and $[M(disacc)_2]^{3-}$ for disaccharide complexes (**7**, **8** and **15**, **16**), where $M = Pr^{3+}$ or Nd^{3+}. Specific hydroxyl groups interacting with the metal centres are derived based on ^{13}C NMR data. All the analytical and spectral information together indicated that the saccharide complexes of Pr(III) and Nd(III) are nine-coordinated as shown through the structures of M–D-glucose (**1**, **9**), Pr–D-ribose, **5**, Nd–D-ribose, **13**, and M–D-maltose (M = Pr or Nd; **7** or **15**) in Fig. 5.

Acknowledgements

C.P.R. acknowledges the Department of Science and Technology, New Delhi, the Department of Atomic Energy, Mumbai, and the

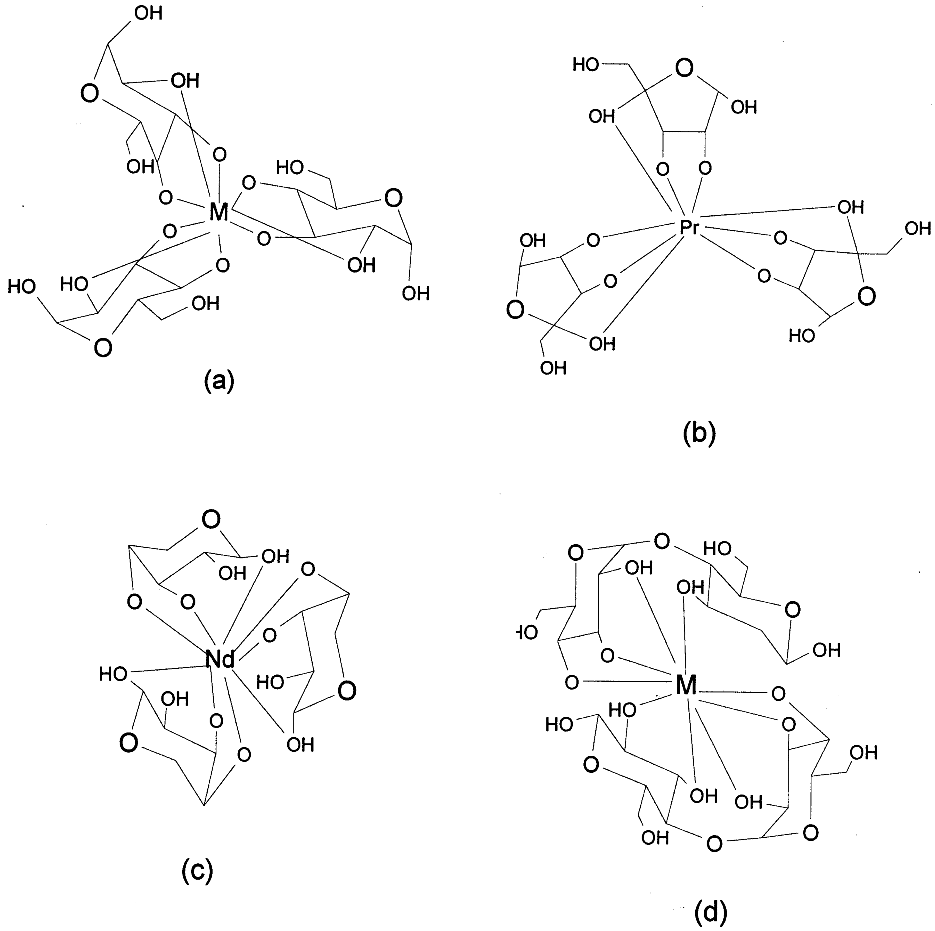

Fig. 5. Schematic representation of the structures of the complexes, (a) M–D-glucose (**1**, **9**); (b) Pr–D-ribose (**5**); (c) Nd–D-ribose (**13**) and (d) M–D-maltose (**7**, **15**) (M = Pr or Nd).

Council of Scientific and Industrial Research, New Delhi, for financial support. The UV-2101 PC was purchased from DST funds. RSIC, IIT-Mumbai is thanked for ICPAES data. We thank Professor S. Mitra, TIFR, Mumbai, for CD measurements. We thank R. Kauppinen, Jyvaskyla University for some experimental help.

References

[1] R.P. Bandwar, C.P. Rao, *Curr. Sci.*, 72 (1997) 788 and references therein.
[2] X. Li, X. Li, S. Zhang, F. Pei, *Polyhedron*, 18 (1999) 685.
[3] Y.M. Wang, Y.J. Wang, R.S. Sheu, G.C. Leu, W.C. Lin, J.M. Liao, *Polyhedron*, 18 (1999) 1147.
[4] A. Mukhopadhyay, E. Kolehmainen, C.P. Rao, *Carbohydr. Res.*, 324 (2000) 30.
[5] W.W. Welender, *J. Inorg. Nucl. Chem.*, 5 (1957) 118.
[6] R.P. Bandwar, C.P. Rao, *Carbohydr. Res.*, 287 (1996) 157.
[7] A. Mukhopadhyay, A. Karkamkar, E. Kolehmainen, C.P. Rao, *Carbohydr. Res.*, 311 (1998) 147.
[8] (a) J.W. Buchler, A.D. Cian, J. Fischer, M.K. Botulinski, R. Weiss, *Inorg. Chem.*, 27 (1988) 339. (b) G.A. Spyroulias, A.G. Coutsolelos, C.P. Raptapoulou, A. Terzis, *Inorg. Chem.*, 34 (1995) 2476. (c) D.H. Zhu, M.J. Kappel, K.N. Raymond, *Inorg. Chim. Acta*, 147 (1988) 115. (d) A. Chisari, A. Musumeci, M. Vidali, A. Seminara, *Inorg. Chim. Acta*, 81 (1984) L19. (e) H. Chen, R.D. Archer, *Inorg. Chem.*, 33 (1994) 5195.
[9] G.H. Dieke, in H.M. Crosswhite, H. Crosswhite (Eds.), *Spectra and Energy Levels of Rare Earth Ions in Crystals*, Wiley, New York, 1968.
[10] (a) S.P. Kaiwar, M.S.S. Raghavan, C.P. Rao, *Carbohydr. Res.*, 256 (1994) 15. (b) A. Sreedhara, M.S.S. Raghavan, C.P. Rao, *Carbohydr. Res.*, 264 (1994) 227. (c) R.P. Bandwar, M.S.S. Raghavan, C.P. Rao, *Biometals*, 8 (1995) 19.
[11] G.A. Spyroulias, C.P. Raptapoulou, D. Montauzon, A. Mari, R. Poilblanc, A. Terzis, A.G. Coutsolelos, *Inorg. Chem.*, 38 (1999) 1683.
[12] R.L. Dutta, S. Shyamal, *Elements of Magnetochemistry*, East–West, India, 1992.
[13] N. Jiazan, S. Feng, L. Zhenxiang, Y. Shaoming, *Inorg. Chim. Acta*, 139 (1987) 165.
[14] C.F.G.C. Geraldes, M.M.C.A. Castro, M.C. Saraiva, M. Aureliano, B.A. Dias, *J. Coord. Chem.*, 17 (1988) 205.

[15] C. Husson, P. Delangle, J. Pecaut, P.J.A. Voettro, *Inorg. Chem.*, 38 (1999) 2012.

[16] (a) G.E. Taylors, J.M. Waters, *Tetrahedron Lett.*, 22 (1981) 1277. (b) K. Tsukagoshi, S. Shinkai, *J. Org. Chem.*, 56 (1991) 4089. (c) M.L.D. Andries, S. Pérez, *Carbohydr. Res.*, 124 (1983) 324. (d) R.E. Lenkinski, J. Ruben, *J. Am. Chem. Soc.*, 98 (1976) 3089. (f) S.J. Angyal, D. Greeves, *Aust. J. Chem.*, 29 (1976) 1223. (g) J. Alfoldi, L. Petrus, V. Bilik, *Coll. Czech. Chem. Commun.*, 43 (1978) 1476. (f) J. Alfoldi, L. Petrus, V. Bilik, *Coll. Czech. Chem. Commun.*, 45 (1980) 123.

[17] (a) R.P. Bandwar, C.P. Rao, *Carbohydr. Res.*, 297 (1997) 341. (b) A. Sreedhara, C.P. Rao, B.J. Rao, *Carbohydr. Res.*, 289 (1996) 39.